

APPLICATION OF NON-CONTACT STRAIN MEASUREMENT TECHNIQUES TO A SINGLE CRYSTAL ALLOY AT ELEVATED TEMPERATURES

D. E. Lempidaki, E. P. Busso and N. P. O'Dowd
Department of Mechanical Engineering, Imperial College London, South Kensington Campus,
London, SW7 2AZ, United Kingdom.

ABSTRACT

Single crystal materials are widely used at elevated temperatures due to their superior high temperature properties. An understanding of the deformation fields in the vicinity of sharp notches and cracks is important in order to identify failure mechanisms for these materials. In this work an optical system used for the measurement of strain fields ahead of notches or cracks in single crystals is described. High temperature tests on stationary cracks were conducted using compact tension single crystal superalloy specimens, within a specially designed furnace that provides optical access to its interior. The method used is digital image correlation whereby the grey value pattern in a predefined area is tracked during deformation using high resolution digital cameras. The full strain fields are then determined as the gradient of the deformation (displacement) field. The strain fields obtained with the optical system are compared to finite element calculations using a rate-dependent crystallographic constitutive framework. Overall, good agreement is obtained, though there are some differences between the predicted and measured strain distributions.

1 INTRODUCTION

The investigation of plastic deformation and strain localisation around notches or cracks in single crystals is important for many reasons. First of all, single crystal materials are used in a number of applications, where high temperature resistance is required. A typical example is the use of single crystal nickel-base superalloys as gas turbine blade materials. On the other hand, polycrystalline materials, which are isotropic at the meso- or macroscale, are composed of a large number of single crystals randomly oriented with respect to each other. Therefore, in order to understand fully the fracture behaviour at the micro-scale and to develop models to predict this behaviour, it is necessary to investigate the deformation around a notch or a crack in a single crystal.

A number of research groups have investigated the deformation ahead of cracks or notches in single crystals. The deformation field around cracks or notches in copper single crystals was investigated using Moiré interferometry (Shield [1], Crone and Shield [2, 3], Crone *et al.* [4]) or electron back-scatter diffraction (Kysar and Briant [5]). These groups have investigated the deformation fields at room temperature. As the materials of interest in this work are widely used at high temperatures, it is important to investigate the deformation fields at these temperatures. In Huimin *et al.* [6] the accumulated creep strain near a hole in a polycrystalline steel plate has been measured using Moiré interferometry (at room temperature). Liu *et al.* [7] have measured the strain fields ahead of a crack in a polycrystalline iron-based alloy at 650°C using digital image correlation (DIC). To the authors' knowledge the strain fields ahead of a crack or notch on a single crystal material have not been studied at temperatures exceeding room temperature. In this work, the strain fields around a notch in a single crystal at 800°C are studied. Measurements are obtained using the DIC technique and compared to finite element (FE) predictions.

2 DEVELOPMENT OF A DIGITAL IMAGE CORRELATION SYSTEM

Surface displacements may be obtained using image correlation by tracking the grey level distribution within a predefined area, which for a digital image comprises a number of pixels (typically 16×16 pixels). This area defines a 'facet' and a data point is determined as the centroid

of the facet. The field of view comprises a number of such facets, (typically 80×64 facets) and the spatial resolution depends on the size of the field of view, which in turn is related to the focal length of the camera lens and the working distance. Digital cameras are used to capture the images within the field of view before and after deformation (image resolution: 1280×1024 pixels) and the deformation and strain fields are determined using image analysis software (ARAMIS, [8]). Two and three-dimensional measurements can be obtained, using one or two cameras, respectively. The values of the field of view and working distance can vary according to the particular measurement (e.g. for a working distance of 330 mm, focal length of 135 mm, the field of view is $13 \times 11 \text{ mm}^2$).

Under certain circumstances, the surface of the specimen may provide sufficient contrast to obtain a measurement without the need for any surface preparation. However, for many materials and applications it is necessary to create a pattern on the surface. A typical pattern is shown in Figure 1, which was obtained by first applying a uniform matte metallic black paint on the specimen surface and then spraying the surface with a white matte metallic paint. However, alternative methods are required to obtain acceptable surface contrast at these temperatures, as discussed in the next section.

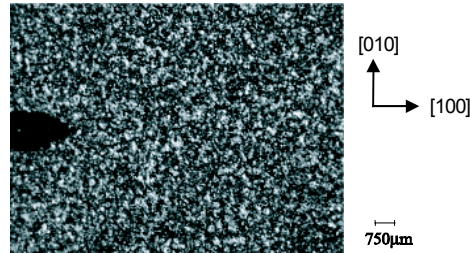


Figure 1: Typical pattern on specimen obtained by spraying white paint on a black background.

The system was optimised and the results validated by room temperature measurements on uniaxial specimens of aluminium and compact tension (CT) specimens of the single crystal Ni-base superalloy, CMSX4. A typical measurement on the CMSX4 alloy is illustrated in Figure 2(a). For this measurement a CT specimen with overall dimensions $32 \times 31 \times 5.5 \text{ mm}^3$, notch depth, $a = 13.3 \text{ mm}$, crack length to specimen width ratio, $a/W = 0.51$ and notch radius $100 \text{ }\mu\text{m}$ was used. The crack plane was (010) and the crack direction was [100] (see Figure 1). The specimen was loaded up to 3.2 kN, (stress intensity factor $K = 36.5 \text{ MPa}\sqrt{\text{m}}$). During loading images were captured at regular intervals using a single camera (eight images in total were obtained).

In Figure 2(a) the total strain normal to the crack face (ε_{22} or $\varepsilon_{[010]}$) is plotted. The field of view is $14 \times 12 \text{ mm}^2$. It is seen in the figure that the peak strain measured is on the order of 0.35% ($3500 \text{ }\mu\varepsilon$) which is below the yield strain of the material measured in a uniaxial test. Some white areas are evident in Figure 2(a), which correspond to regions where there was not sufficient contrast within the facet to obtain a strain measurement. The notch geometry is shown in Figure 2(a) as an inset to the measurement. Note that it is not possible to obtain readings very close to the notch due to the limited number of data points there.

The measurements obtained using the DIC system have been compared to finite element calculations conducted on a 3-D mesh of a CT specimen, as shown in Figure 3. In this analysis it is assumed that the specimen and notch are perfectly aligned so two axes of symmetry exist and only one quarter of the specimen is analysed.

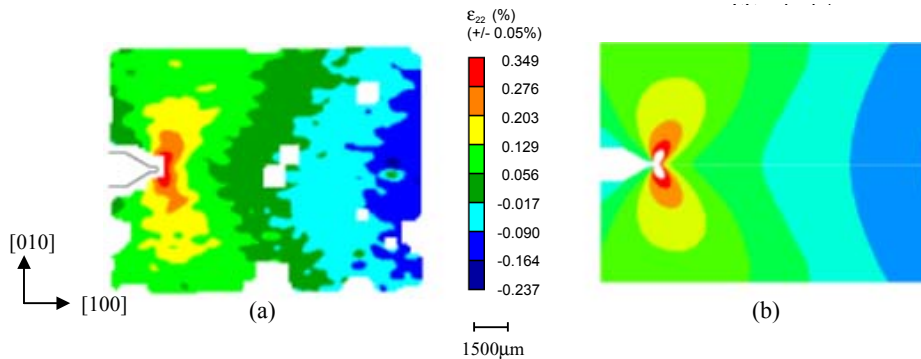


Figure 2: Comparison between (a) DIC measurement at room temperature and (b) FE calculation.

A total of 6,300 eight noded, linear, three dimensional elements (C3D8) were used and the mesh has approx. 25,000 degrees of freedom in total. For this analysis, the material is assumed to remain elastic and as the CMSX4 material has cubic symmetry only three elastic constants are required. These have been obtained from Dennis [9] and are given as tensile modulus, $E_{[100]} = 122$ GPa, shear modulus, $G_{[100]} = 131$ GPa and Poisson ratio, $\nu_{[100]} = 0.365$. The analysis has been carried out using the finite element package ABAQUS [10].

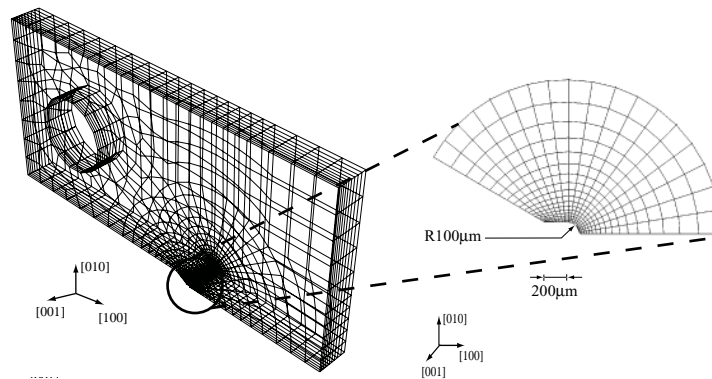


Figure 3: Three-dimensional mesh used for finite element calculations.

The result from the finite element analysis is shown in Figure 2(b). The excellent agreement between the measurement and the finite element prediction is evident. To illustrate the comparison between the measured and predicted strains more directly, the strains normal to the crack face have been plotted against distance from the crack tip in Figure 4. Taking into consideration the quoted strain resolution of the DIC system, which is indicated by the error bar in Figure 4, the measured and predicted strains are in agreement, with the measured strains somewhat higher than those predicted by the FE analysis (though within the quoted resolution of the system). Again, the gap in the measured strain distribution at a distance of approx. 6 mm from the notch tip is due to a number of invalid facets in this region.

3 HIGH TEMPERATURE MEASUREMENTS

Measurement of the strain field was conducted on CT specimens of CMSX4 at 800°C within a specially designed furnace providing optical access to the interior. The specimen geometry was the same as that used for the low temperature measurements. In this case, in order to obtain a contrast,

which would be sustained at high temperature, a special surface preparation was required. The specimen surface was first oxidised at 800°C for 72 hours to obtain a suitable dark background due to the formation of an oxide layer. A white particle distribution was then produced by spraying the surface with a titania ethanol mixture. Further details of the preparation method are provided in Lempidaki *et al.* [11]. The CT specimen was loaded up to 8 kN ($K = 91.3 \text{ MPa}\sqrt{\text{m}}$) and the specimen was held at maximum load for 5 hours at 800°C.

3.1 DIC Measurements

For the high temperature measurements the specimen is placed in a furnace which sets a minimum working distance for the camera(s). For this measurement a single camera was used with a working distance of 330 mm giving a field of view of $13 \times 11 \text{ mm}^2$ and a facet size of approx. $0.2 \times 0.2 \text{ mm}^2$. The strain field obtained from the DIC measurements is shown in Figure 5(a). It may be seen that the peak strains are 3.6% ($36,000 \mu\epsilon$), which is well outside the linear elastic regime for this material. It should be noted that even though the dwell period was only 5 hours significant creep strains have accumulated over this period.

3.2 Finite Element Predictions

To allow comparison between the measured and predicted strains the material model must take into account the non-linear, rate dependent response of CMSX4 at elevated temperatures. The crystallographic-based CMSX4 material model developed by Dennis [9] has therefore been used. In this model, the inelastic deformation in the single crystal alloy occurs by deformation on favourable slip systems. At the relevant temperatures, the operating slip systems for CMSX4 are the cubic ($\{100\}\langle 011\rangle$) slip systems in addition to the octahedral ($\{111\}\langle 011\rangle$) systems.

The proposed crystallographic formulation relies on the multiplicative decomposition of the total deformation gradient \mathbf{F} into an elastic part \mathbf{F}^e , which accounts for the elastic stretching and rigid-body rotations and an inelastic part, \mathbf{F}^p , which is associated with pure slip, thus

$$\mathbf{F} = \mathbf{F}^e \mathbf{F}^p, \quad (1)$$

Elastic deformation has cubic symmetry, and the inelastic deformation is determined by the accumulation of slip on the relevant CMSX4 slip systems. Thus the inelastic strain rate, \mathbf{L}^p , is determined as,

$$\mathbf{L}^p = \dot{\mathbf{F}}^p (\mathbf{F}^p)^{-1} = \sum_{\alpha=1}^n \dot{\gamma}^{\alpha} (\mathbf{m}^{\alpha} \otimes \mathbf{n}^{\alpha}), \quad (2)$$

where $\dot{\gamma}^{\alpha}$ is the strain rate on the slip system α and \mathbf{m}^{α} and \mathbf{n}^{α} are the slip direction and slip plane normal, respectively. Further details of the large strain kinematics of the model can be found in Dennis [9], Dumoulin *et al.* [12] and Zhao *et al.* [13].

The flow rule is based on a stress-dependent activation energy and is expressed in terms of two internal variables per slip system α : a macroscopically slip resistance S^{α} and a back stress B^{α} . The inelastic strain rate on a slip system α , is given by,

$$\dot{\gamma}^{\alpha} = \dot{\gamma}_0 \exp \left[-\frac{F_0}{kT} \left(1 - \left(\frac{|\tau^{\alpha} - B^{\alpha}| - S^{\alpha} \mu / \mu_0}{\tau_0 \mu / \mu_0} \right)^p \right)^q \right] \text{sgn}(\tau^{\alpha} - B^{\alpha}), \quad (3)$$

where k is the Boltzmann constant, τ^{α} is the resolved shear stress on the slip system α , T the absolute temperature, μ , μ_0 the shear moduli at the current temperature and 0 K respectively, and F_0 , τ_0 , p , q and $\dot{\gamma}_0$ are material constants.

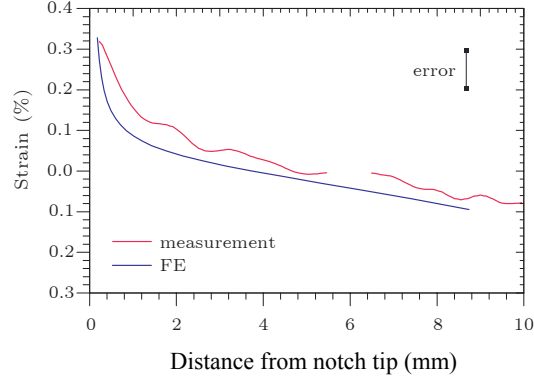


Figure 4: Comparison of strains ahead of the crack tip between measurement and FE calculation.

The slip resistance, S , and back stress, B , are given by,

$$\dot{S}^\alpha = (h_s - d_s(S^\alpha - S_0^\alpha))|\dot{\gamma}^\alpha|; \quad \dot{B}^\alpha = h_B\dot{\gamma}^\alpha - d_B B^\alpha|\dot{\gamma}^\alpha|. \quad (4)$$

In Eq. (4) S_0^α is the initial slip resistance and is microstructurally dependant (size and volume fraction of the γ precipitates) and h_s , h_B , d_s , d_B are material constants, which depend on microstructure and temperature. The material constants have been calculated based on experimental and unit cell studies on representative microstructures, (Meissonnier *et al.* [14]).

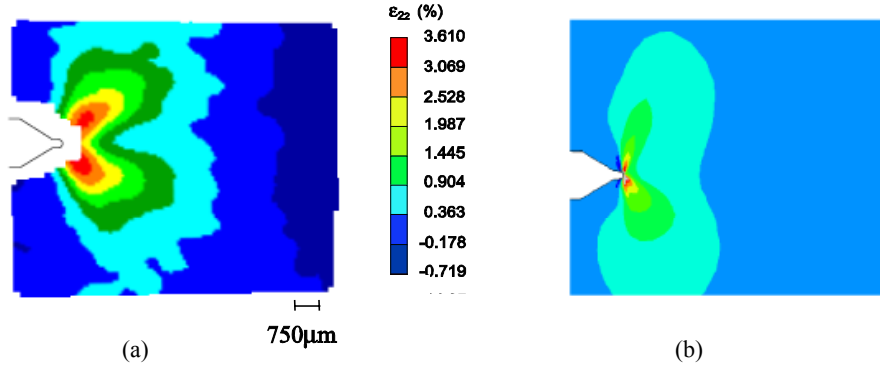


Figure 5: Strain distribution after 5 hours at 800°C (a) DIC measurement (b) FE prediction.

Finite element calculations were conducted using the mesh shown in Figure 3 following the test program described in the previous sections. The results are shown in Figure 5(b). Note that the strain contours in the FE analysis are somewhat asymmetric about the notch plane due to the fact that the specimen is not precisely aligned along the [010] direction. The overall magnitude of strain predicted by the FE analysis is in general agreement with the measured values. However, the predicted region of peak strain is of smaller size to that measured. The reason for the discrepancy between the model predictions and the measured strain at high temperatures is under investigation.

4 CONCLUSIONS

An optical system has been developed for measurement of strain fields using digital image correlation. A specially designed furnace provides optical access to its interior, such that in-situ strain measurement is feasible at high temperature. Measured strain fields at room temperature and 800°C are compared to finite element calculations using a rate dependent crystallographic model.

Excellent agreement has been obtained between the room temperature measurements and linear elastic finite element predictions. Some discrepancies between the measured and predicted strain distributions at 800°C have been identified and are under investigation.

5 REFERENCES

1. Shield, T.W. “An Experimental Study of the Plastic Strain Fields Near a Notch tip in a Copper Single Crystal During Loading”, *Acta Materialia*, **44**, 1547–1561, 1996.
2. Crone W.C. and Shield T.W., “Experimental Study of the Deformation near a Notch Tip in Copper and Copper – Beryllium Single Crystals”, *Journal of the Mechanics and Physics of Solids*, **49**, 2819 – 2838, 2001.
3. Crone W.C. and Shield T.W., “An Experimental Study of the Effect of Hardening on Plastic Deformation at Notch Tips in Metallic Single Crystals”, *Journal of the Mechanics and Physics of Solids*, **51**, 1623 – 1647, 2003.
4. Crone W.C., Shield T.W., Creuziger, A. and Henneman, B. “Orientation Dependence of the Plastic Slip near Notches in Ductile FCC Single Crystals”, *Journal of the Mechanics and Physics of Solids*, **52**, 85 – 112, 2004.
5. Kysar, J.W. and Briant C.L., “Crack-Tip Deformation Fields in Ductile Single Crystals”, *Acta Materialia*, **50**, 2367 – 2380, 2002.
6. Huimin, X., Fulong, D., Dietz, P. Schmidt, A. and Wei, Z. “600°C Creep Analysis of Metals Using the Moire interferometry method”, *Journal of Materials Processing Technology*, **88**, 185 – 189, 1999.
7. Liu, J., Sutton, M., Lyons, J. and Deng, X. “Experimental investigation of Near Crack Tip Deformation in alloy 800 at 650°C”, *International Journal of Fracture*, **91**, 233-268, 1998.
8. ARAMIS User Handbook, GOM mbH, Braunschweig, Germany, 2001.
9. Dennis, R.J., Mechanistic Modelling of Deformation and Void Growth Behaviour in Superalloy Single Crystals, PhD thesis, Imperial College London, 2000.
10. ABAQUS version 6.2. Hibbitt, Karlsson and Sorensen, Inc., 2001.
11. Lempidaki, D.E., Busso, E.P. and O’Dowd, N.P., “Non-Contact Measurement of Strain Localisation around Notches in Single Crystals”, work in preparation, 2004.
12. Dumoulin, S., Busso, E.P. and O’Dowd, N.P. “A Multiscale Approach for Coupled Phenomena in FCC Materials at High Temperatures”, *Philosophical Magazine*, **83** 3895–3916, 2003.
13. Zhao, L.G., O’Dowd, N.P. and Busso, E.P. “A Coupled Approach to the Study of High Temperature Crack Initiation in Single Crystal Superalloys”, work in preparation, 2004.
14. Meissonnier, F., Busso, E.P. and O’Dowd, N.P., “Finite Element Implementation of a Generalised Non-Local Rate Dependent Crystallographic Formulation for Finite Strains”, *International Journal of Plasticity*, **17**, 601– 640, 2001.